



Published in final edited form as:

Polym Chem. 2014 ; 5(5): 1581–1585. doi:10.1039/C3PY01245J.

Anticancer Camptothecin-*N*-Poly(lactic acid) Nanoconjugates with Facile Hydrolysable Linker

Qian Yin^a, Rong Tong^{a,b}, Lichen Yin^a, Timothy M. Fan^c, and Jianjun Cheng^{a,*}

^aDepartment of Materials Science and Engineering, University of Illinois at Urbana–Champaign, Urbana, IL 61801 (USA)

^cDepartment of Veterinary Clinical Medicine, University of Illinois at Urbana-Champaign, Urbana, Illinois 61801, USA

Abstract

We report a strategy of conjugating CPT to the terminal carboxylate group of polylactide (PLA) with a facile hydrolysable amino ester linker via a controlled polymerization method. The obtained CPT-*N*-PLA conjugates were able to self-assemble into 50-100 nanometer-sized conjugates (NCs) with desired *in vitro* physicochemical properties and showed enhanced *in vivo* therapeutic efficacy against Lewis lung carcinoma (LLC) induced in C57BL/6 mice.

Introduction

20(*S*)-Camptothecin (CPT), a topoisomerase I inhibitor isolated from the Chinese tree *Camptotheca acuminata* in the 1960s, has been demonstrated to have a broad range of remarkable anticancer activities against various tumor models.^{1, 2} However, the low aqueous solubility of its therapeutically active lactone form has largely hindered its clinical applications. When placed in an aqueous solution at physiological pH, CPT is quickly transformed from its therapeutically active lactone form to inactive carboxylate form, leading to severe toxicity. Additionally, favorable binding with serum albumin of the carboxylate form of CPT forces lactone-carboxylate equilibrium toward the formation of the carboxylate.³⁻⁵ Furthermore, CPT tends to be quickly eliminated from the circulation system after being intravenously administered because of its low molecular weight, which significantly diminishes its anticancer activity. To circumvent these drawbacks, there are numerous efforts for synthesizing CPT analogues to achieve improved solubility and enhanced lactone stability.⁶⁻⁹

Polymeric nanomedicine, an emerging field that includes the use of drug-containing polymeric nanoparticles (NPs), opens up a new opportunity for overcoming the shortcomings of CPT.¹⁰⁻¹⁴ Utilizing polymeric NPs as drug carriers to deliver CPT has potential to provide various benefits like improved water solubility, reduced clearance,

© The Royal Society of Chemistry [year]

*jianjunc@illinois.edu.

^bCurrent address: Department of Chemical Engineering, Massachusetts Institute of Technology, Cambridge, Massachusetts 02139, USA.

reduced drug resistance and enhanced therapeutic effectiveness.¹⁵⁻¹⁷ Poly(lactic acid) (PLA) is one of the extensively used polymeric materials in the formulation of NPs due to its excellent safety profile, tunable degradation kinetics and ease of synthesis.^{18, 19} PLA NPs that encapsulate CPT can be readily prepared via co-precipitation of polymer and drug.^{20, 21} However, such encapsulation method tends to bring several formulation issues of NPs, such as low encapsulation efficiency, low drug loading, heterogeneous compositions, and “burst” drug release profile, which highly impact their pharmacological and pharmacokinetic properties *in vivo*.^{20, 22}

To address these challenges, we previously developed CPT-PLA nanoconjugates (NCs) through CPT-initiated ring-opening polymerization (ROP) of lactide (LA) followed by nanoprecipitation of the resulting CPT-PLA conjugates.²³ CPT-PLA NCs possess some properties like nearly 100% loading efficiency, tunable drug loading, and narrowly distributed particle sizes. In these NCs, the release of CPT is attributed to the cleavage of a lactate ester bond between CPT and PLA through hydrolysis at physiological conditions.²³ Because PLA is hydrophobic, the entanglement of polymer chain forms rigid core of NCs. Water and ions (e.g., H⁺ and OH⁻) were not able to access to the ester linkage easily and therefore results in slow release kinetics of CPT: only 50% of CPT is released from conjugates in PBS after two weeks at 37 °C.²³ Such slow release profile can significantly diminish the side effects of free CPT in circulation, brings difficulty to achieve the active drug concentration within short time in tumors. To improve the efficacy of CPT-PLA NCs, an improved rapid release of CPT from NC, while still avoiding burst release, is desired. As reported, amine could accelerate the hydrolysis of esters by facilitating to form a destabilized intermediate during the hydrolysis process.²⁴ Thus, we report a simple chemistry that allows for facile conjugation of CPT to the terminal carboxylate group of polylactide (PLA) via a hydrolysis-labile amino ester linker. Instead of using poorly controlled coupling chemistry, we developed a ring-opening polymerization (ROP) method to facilitate the incorporation of hydrophilic amino ester linker between CPT and PLA. The obtained CPT-*N*-PLA conjugates were able to be co-precipitated with methoxy-poly(ethylene glycol)-PLA (mPEG-PLA) to self-assemble into NCs with well-controlled physicochemical properties, such as sub-100 nm size, narrow size distribution and controlled release kinetics. We also demonstrated that the formulated NCs with rapid drug release kinetic profile could potentially enhance the *in vivo* therapeutic efficacy against Lewis lung carcinoma (LLC) induced in C57BL/6 mice.

Results and Discussion

Synthesis and characterization of CPT-*N*-LA_{*n*} conjugates

It has been suggested that the release of conjugated anticancer drug should occur in a controlled manner within the tumor stroma to maximize its therapeutic efficacy and the drug-oligomer conjugates formed by the hydrolysis of polymer chains during the circulation should be inhibited to minimize the systemic toxicity.²⁵ Thus, distinctive differences of hydrolysis rates between drug-polymer and polymer backbones are desirable. To achieve this aim, the CPT derivative was first synthesized by condensation of bromoacetic acid with CPT's C20-hydroxyl group to yield CPT-bromide (CPT-Br). Then, CPT-Br was reacted

with ethanolamine to obtain *N*-substituted CPT-ester containing primary hydroxyl group, termed CPT-*N*-OH. As we previously reported, the pendent hydroxyl group of the therapeutic agent allows for one-step drug conjugation to the terminal carboxylate group of PLA via a ROP method facilitated by BDI-Zn catalyst.^{23, 26-28} Through such living polymerization, both the initiation (CPT-*N*-OH incorporation) and the chain propagation can proceed in a well-controlled manner and result in materials with pre-defined drug loadings and narrow molecular weight distributions (MWDs) (Figure 1).

Controlled ROP were performed over a broad range of LA/CPT-*N*-OH ratios from 10 to 200 when the LA polymerizations were mediated by (BDI-EI)ZnN(TMS)₂/CPT-*N*-OH with quantitative CPT-*N*-OH incorporation efficiencies and narrow MWDs ($M_w/M_n = 1.09-1.23$) (Table 1). The obtained MWs of the CPT-*N*-PLA_n conjugates were in excellent agreement with the expected MWs, which followed a linear correlation with the LA/CPT-*N*-OH ratios (Figure 2B). Monomodal GPC MW distribution curves were observed in all CPT-*N*-PLA_n conjugates prepared with various LA/CPT-*N*-OH ratios (Figure 2A). The well-controlled polymerization mediated by (BDI-EI)ZnN(TMS)₂/CPT-*N*-OH presumably proceeded through the insertion-coordination mechanism as reported.²³

Preparation and characterization of CPT-*N*-LA₁₀ NC

Nanoprecipitation, representing a facile, non-extensive and low-energy consuming technique has been widely used for the preparation of versatile polymeric NPs.^{22, 29-31} In this study, the CPT-*N*-PLA conjugate was dissolved in water-miscible organic solvent (DMF) and then dropwise added into fast stirring water, resulting in formation of CPT-*N*-PLA₁₀ NCs with CPT embedded in the hydrophobic PLA matrices (Table 2). This method allows for a rapid production of NC with sub-100 nm size and very narrow size distribution in a large quantity (gram scale), which confirmed with dynamic light scattering (DLS) (Figure 3A). Furthermore, the sizes of these NCs prepared by nanoprecipitation can be easily controlled by tuning the concentration of polymer.²² When the DMF/water ratio is fixed at 1/20 (v/v), the size of CPT-*N*-PLA₁₀ NCs showed a linear correlation with the concentration of CPT-*N*-PLA₁₀ conjugate and can be precisely tuned from 50 nm to 75 nm (Figure 3B).

To achieve favorable *in vivo* performance, the NCs are expected to have prolonged circulation time to maximize their therapeutic efficacy.³²⁻³⁴ However, surface-unmodified NC are usually found to have non-specific binding with proteins in blood to form large aggregates, subsequently resulting in rapid clearance from the blood stream due to uptake by the reticuloendothelial systems (RES).³⁵ Modification of NC surfaces with PEG, termed “PEGylation”, is the most widely used approach to reduce recognition by RES and prolong systemic circulation.³⁶ To minimize efforts for complicated chemical synthesis, we applied a facile strategy to coat the surface of NCs with PEG. By mixing mPEG_{5k}-PLA₁₀ (PLA block of 1.4 kDa and mPEG segment of 5 kDa) copolymer with CPT-*N*-PLA₁₀ conjugate followed by nanoprecipitation technique, it yields PEGylated NCs via the hydrophobic interaction of PLA segments of mPEG_{5k}-PLA₁₀ and CPT-*N*-PLA₁₀. As shown in Figure 3D, the nanoparticle size in water increased from 73 to 93 nm after PEGylation, indicating that PEGylation only partly contributed to the increased particle diameter. When dispersed in

PBS, cell culture medium (DMEM) and human serum, the particle size was further augmented by 20–40 nm, which was presumably attributed to the salt-induced screening of the repulsive force.²² No aggregation was noted according to the DLS histogram, which demonstrated the desired stability of the PEGylated CPT-*N*-PLA₁₀ NC (Figure 3C). For further clinical applications, it is desirable that NCs formulated in solid form that bear with their original well-controlled properties, feasible for the long-term storage and transport prior to their use in clinic.³⁷ As shown in Figure 3D, bovine serum albumin (BSA), a ubiquitous protein in the blood, could be used to stabilize CPT-*N*-PLA₁₀ NC and effectively prevent the severe aggregation of NCs during lyophilization process.²²

Drug release kinetics and cytotoxicity

We performed the release kinetic study of CPT from PEGylated CPT-*N*-LA₁₀ NC and PEGylated CPT-LA₁₀ NC respectively in the 50% human serum buffer, which better mimics the release in physiological conditions. Since the release kinetics of CPT is determined by the hydrolysis of ester linkage between CPT and NCs, the release kinetics of CPT from NCs are more sustainable as compared to the burst release profile often observed in the polymeric encapsulates. As shown in Figure 4A, CPT-LA₁₀ NC with the hydrophobic ester linker between CPT and polymeric NC exhibited sustained drug release with 18% CPT released over 48 h. In comparison, when the linker changed to hydrolysis-labile amino ester linker, the release kinetics of CPT from CPT-*N*-LA₁₀ NC could be significantly accelerated with nearly 50% CPT being released within the same period of time. *In vitro* toxicity of NCs is highly correlated with the amount of drug released from NCs, we therefore evaluated the cytotoxicity of PEGylated CPT-LA NCs with two different linkers in MCF-7 cells using MTT assay (Figure 4B). The IC₅₀ of PEGylated CPT-LA₁₀ NC (1435 nM) is nearly three times higher than PEGylated CPT-*N*-LA₁₀ NC (454 nM). As a result, the toxicity of PEGylated CPT-NCs against cancer cell proliferation could be improved simply by controlling the linker.

In vivo efficacy of CPT-*N*-LA NCs

We infer that the NC formulation with rapid drug release kinetic profile will potentially enhance the efficacy. For proof of concept, we then investigated the *in vivo* therapeutic efficacy of NCs against Lewis lung carcinoma (LLC) induced by subcutaneous injection of LLC cells into the C57BL/6 mice. The study protocol was reviewed and approved by the Illinois Institutional Animal Care and Use Committee (IACUC) of University of Illinois at Urbana–Champaign (see the ESI[†] for further details). When the size of tumors reached around 200 mm³, the mice were divided to five groups to minimize the differences of body weights and tumor sizes among groups (N=6). Two groups of mice received the single intravenous injection of PEGylated CPT-*N*-LA₁₀ NC and PEGylated CPT-LA₁₀ NC at the dose of 50 mg CPT per kg mice body weight (50 mg/kg), respectively. Irinotecan, a CPT analogue with improved solubility, was administrated as clinically suggested at the single dose of 100 mg/kg intravenously. The other two groups were administrated intravenously with PBS and mPEG-PLA NC as negative controls (Figure 5A). The tumor sizes and body

[†]Electronic Supplementary Information (ESI) available: [Experimental procedures, FT-IR spectra and MALDI-TOF MS analysis of synthesized drug-polymer conjugates]. See DOI: 10.1039/b000000x/

weights of mice in each group were monitored continuously for 8 days post injection. We found the group of mice treated with PEGylated CPT-*N*-LA₁₀ NCs significantly delayed of tumor growth and more effective than groups treated with CPT-LA₁₀ NCs, and other control groups ($P < 0.05$, Mann-Whitney U test, Figure 5B and 5C). Our efficacy result is further confirmed by TUNEL staining of tumor sections obtained from above five groups of mice at day 8. As shown in Figure 5E, tumors treated with CPT-*N*-LA₁₀ NCs had substantially increased the apoptotic cell numbers compared with those treated with CPT-LA₁₀ NCs. The apoptotic index (TUNEL/DAPI, day 8) indicates that CPT-*N*-LA₁₀ NC (12.29%) showed dramatically improved efficacy compared to the CPT-LA₁₀ NC (9.23%) (Figure 5E). When evaluating the body weight changes of all the mice received treatments, none significant (<20%) body weight drop was observed (Figure 5D), which indicated minimal acute toxicities of CPT-loaded polymeric NCs.

Conclusions

Overall, by taking advantage of the controlled ROP method, we successfully designed and incorporate a hydrolysis-labile amino ester linker to conjugated CPT to PLA with via a fully controlled manner. The resulting CPT-*N*-PLA conjugates were able to self-assemble into sub-100nm-sized NCs with desired physicochemical properties, with accelerated release kinetics compared with our previous CPT-PLA NCs. We also demonstrated such improvement could contribute to the enhanced *in vivo* efficacy: the growth of Lewis lung carcinomas (LLCs) induced in C57BL/6 mice was significantly delayed compared with CPT-PLA NCs, without acute systemic toxicity.

Supplementary Material

Refer to Web version on PubMed Central for supplementary material.

Acknowledgements

This work was supported by National Science Foundation (Career Program DMR-0748834 and DMR-1309525) and the National Institute of Health (NIH Director's New Innovator Award 1DP2OD007246-01; 1R21CA152627). Q.Y. was funded at UIUC from NIH National Cancer Institute Alliance for Nanotechnology in Cancer "Midwest Cancer Nanotechnology Training Center" Grant R25 CA154015A.

Notes and references

1. Liu LF, Desai SD, Li TK, Mao Y, Sun M, Sim SP. *Ann Ny Acad Sci.* 2000; 922:1–10. [PubMed: 11193884]
2. Gallo RC, Whangpen J, Adamson RH. *J Natl Cancer I.* 1971; 46:789.
3. Li QY, Zu YG, Shi RZ, Yao LP. *Curr Med Chem.* 2006; 13:2021–2039. [PubMed: 16842195]
4. Mi ZH, Burke TG. *Biochemistry-U.S.* 1994; 33:10325–10336.
5. Mi ZH, Burke TG. *Biochemistry-U.S.* 1994; 33:12540–12545.
6. Bissery MC, Vrignaud P, Lavelle F, Chabot GG. *Anti-Cancer Drug.* 1996; 7:437–460.
7. Staker BL, Hjerrild K, Feese MD, Behnke CA, Burgin AB, Stewart L. *P Natl Acad Sci USA.* 2002; 99:15387–15392.
8. Muggia FM, Dimery I, Arbuck SG. *Ann Ny Acad Sci.* 1996; 803:213–223. [PubMed: 8993515]
9. Lu H, Lin HX, Jiang Y, Zhou XG, Wu BL, Chen JM. *Lett Drug Des Discov.* 2006; 3:83–86.
10. Tong R, Cheng J. *Polymer Reviews.* 2007; 47:345–381.

11. Yin Q, Tong R, Xu YX, Baek K, Dobrucki LW, Fan TM, Cheng JJ. *Biomacromolecules*. 2013; 14:920–929. [PubMed: 23445497]
12. Bhatt RL, de Vries P, Tulinsky J, Bellamy G, Baker B, Singer JW, Klein P. *J Med Chem*. 2003; 46:190–193. [PubMed: 12502373]
13. Yu MK, Park J, Jon S. *Theranostics*. 2012; 2:3–44. [PubMed: 22272217]
14. Me ZG, Lu TC, Chen XS, Zheng YH, Jing XB. *J Biomed Mater Res A*. 2009; 88A:238–245.
15. Langer R. *Nature*. 1998; 392:5–10. [PubMed: 9579855]
16. Cheng J, Khin KT, Davis ME. *Mol Pharmaceut*. 2004; 1:183–193.
17. Schluep T, Hwang J, Cheng JJ, Heidel JD, Bartlett DW, Hollister B, Davis ME. *Clin Cancer Res*. 2006; 12:1606–1614. [PubMed: 16533788]
18. Oh JK. *Soft Matter*. 2011; 7:5096–5108.
19. Xu XL, Chen XS, Wang ZF, Jing XB. *Eur J Pharm Biopharm*. 2009; 72:18–25. [PubMed: 19027067]
20. Cheng J, Teply BA, Sherifi I, Sung J, Luther G, Gu FX, Levy-Nissenbaum E, Radovic-Moreno AF, Langer R, Farokhzad OC. *Biomaterials*. 2007; 28:869–876. [PubMed: 17055572]
21. Bendix D. *Polym Degrad Stabil*. 1998; 59:129–135.
22. Tong R, Yala LD, Fan TM, Cheng JJ. *Biomaterials*. 2010; 31:3043–3053. [PubMed: 20122727]
23. Tong R, Cheng JJ. *Bioconjugate Chem*. 2010; 21:111–121.
24. Bender ML, Turnquest BW. *J Am Chem Soc*. 1957; 79:1656–1662.
25. Larson N, Ghandehari H. *Chem Mater*. 2012; 24:840–853. [PubMed: 22707853]
26. Tong R, Cheng JJ. *Macromolecules*. 2012; 45:2225–2232. [PubMed: 23357880]
27. Tong R, Cheng JJ. *Angew Chem Int Edit*. 2008; 47:4830–4834.
28. Tong R, Cheng JJ. *J Am Chem Soc*. 2009; 131:4744–4754. [PubMed: 19281160]
29. Chen CY, Kim TH, Wu WC, Huang CM, Wei H, Mount CW, Tian YQ, Jang SH, Pun SH, Jen AKY. *Biomaterials*. 2013; 34:4501–4509. [PubMed: 23498892]
30. Zhao Z, Wang J, Mao HQ, Leong KW. *Adv Drug Deliver Rev*. 2003; 55:483–499.
31. Farokhzad OC, Cheng JJ, Teply BA, Sherifi I, Jon S, Kantoff PW, Richie JP, Langer R. *P Natl Acad Sci USA*. 2006; 103:6315–6320.
32. Kim D, Park S, Lee JH, Jeong YY, Jon S. *J Am Chem Soc*. 2007; 129:7661–7665. [PubMed: 17530850]
33. Moghimi SM, Hunter AC, Murray JC. *Pharmacol Rev*. 2001; 53:283–318. [PubMed: 11356986]
34. Burke RS, Pun SH. *Bioconjugate Chem*. 2008; 19:693–704.
35. Wagner V, Dullaart A, Bock AK, Zweck A. *Nat Biotechnol*. 2006; 24:1211–1217. [PubMed: 17033654]
36. Roberts MJ, Bentley MD, Harris JM. *Adv Drug Deliver Rev*. 2002; 54:459–476.
37. Musumeci T, Vicari L, Ventura CA, Gulisano M, Pignatello R, Puglisi G. *J Nanosci Nanotechnol*. 2006; 6:3118–3125.

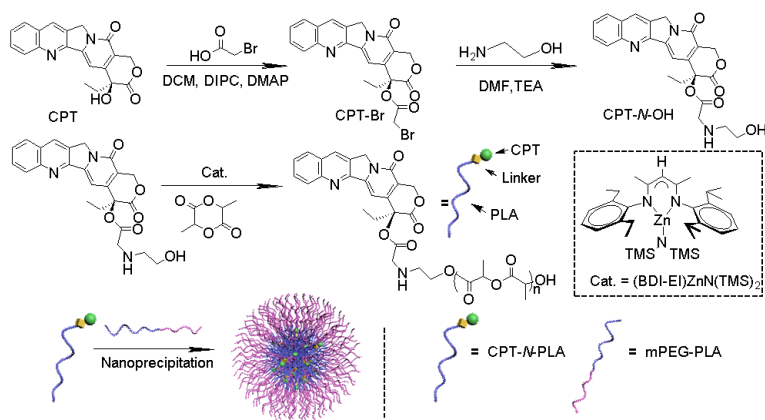


Figure 1. Preparation of PEGylated CPT-N-PLA NCs via CPT-N-OH initiated LA polymerization in the presence of $(\text{BDI-EI})\text{ZnN}(\text{TMS})_2$, followed by nanoprecipitation and non-covalent surface modification.

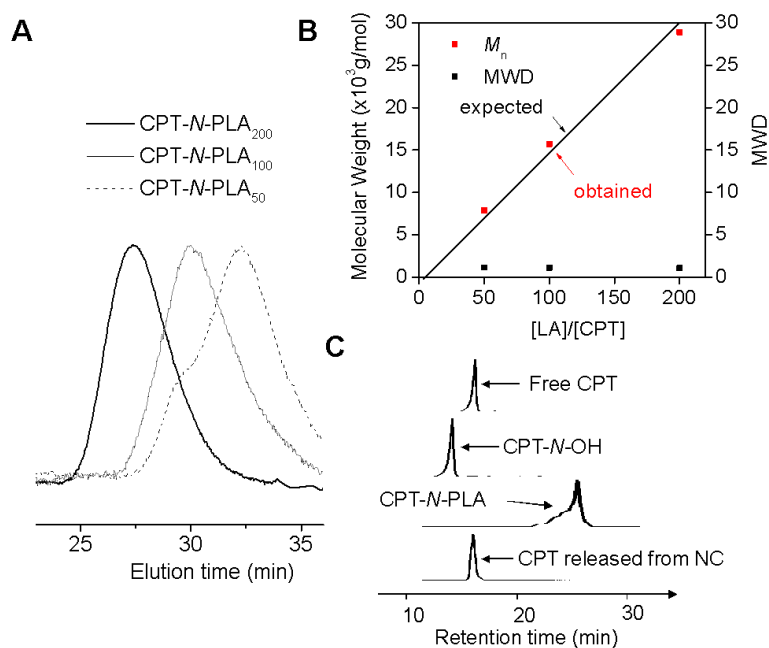


Figure 2. (A) Overlay of GPC traces of CPT-*N*-PLA_{*n*} (*n* = 50, 100 and 200). (B) (BDI-EI)ZnN(TMS)₂/CPT mediated controlled ring-opening polymerization (ROP) of LA at various ratio of LA/CPT (MWD = Molecular Weight Distribution). (C) HPLC analysis of CPT-*N*-OH initiated polymerization and release of CPT from CPT-*N*-PLA_{*n*} NC. (HPLC traces from top to bottom: free CPT, CPT-*N*-OH, CPT-*N*-PLA, CPT released from CPT-*N*-PLA NC).

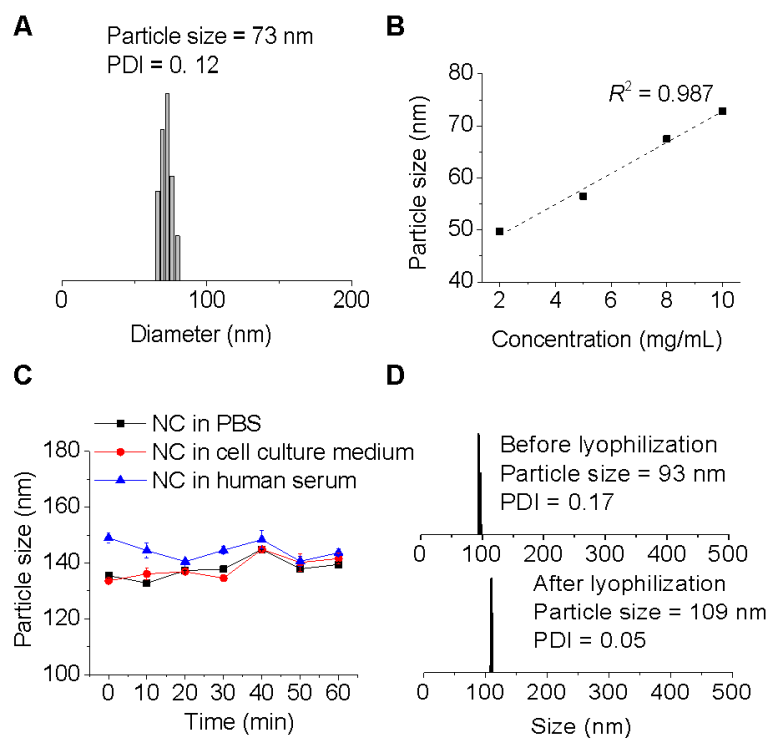


Figure 3. Formulation and characterization of CPT-*N*-PLA₁₀ NCs. (A) DLS analysis of CPT-*N*-PLA₁₀ NC in water (0.5 mg/mL). (B) Precipitation of CPT-*N*-PLA₁₀ from DMF solution into water at various CPT-*N*-PLA₁₀ concentrations. (C) Stability of PEGylated CPT-*N*-PLA₁₀ NCs in PBS, cell culture medium, and human serum buffer (human serum:PBS=1:1, v/v). (D) DLS analysis of NCs reconstitution: Monodispersed PEGylated CPT-*N*-PLA₁₀ NCs mixed with bovine serum albumin (BSA) in water before lyophilization (upper panel). The reconstituted NC after lyophilization in the presence of BSA (BSA:NC=10:1, wt/wt) (bottom panel).

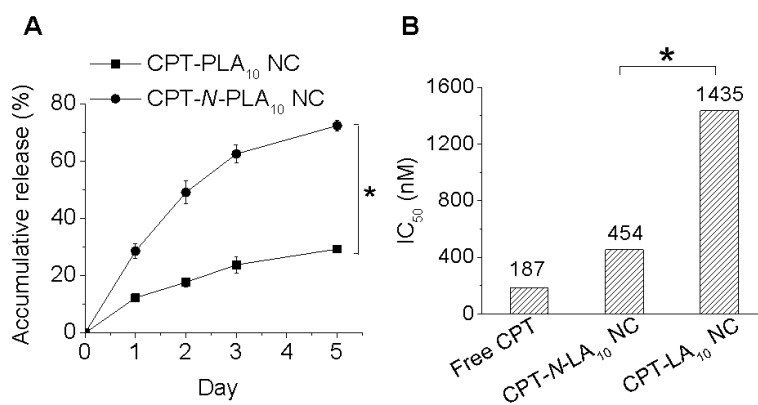


Figure 4. (A) Release kinetics of CPT from PEGylated CPT-PLA₁₀ NC and PEGylated CPT-N-PLA₁₀ NC in human serum buffer (human serum:PBS=1:1, v/v) at 37 °C. (B) Cytotoxicity of free CPT, PEGylated CPT-LA₁₀ NC and PEGylated CPT-N-PLA₁₀ in MCF-7 cells as determined by MTT assay (37 °C, 72 h). Statistical differences between the groups were assessed with Student's t-test. * $P < 0.05$ is considered statistically significant.

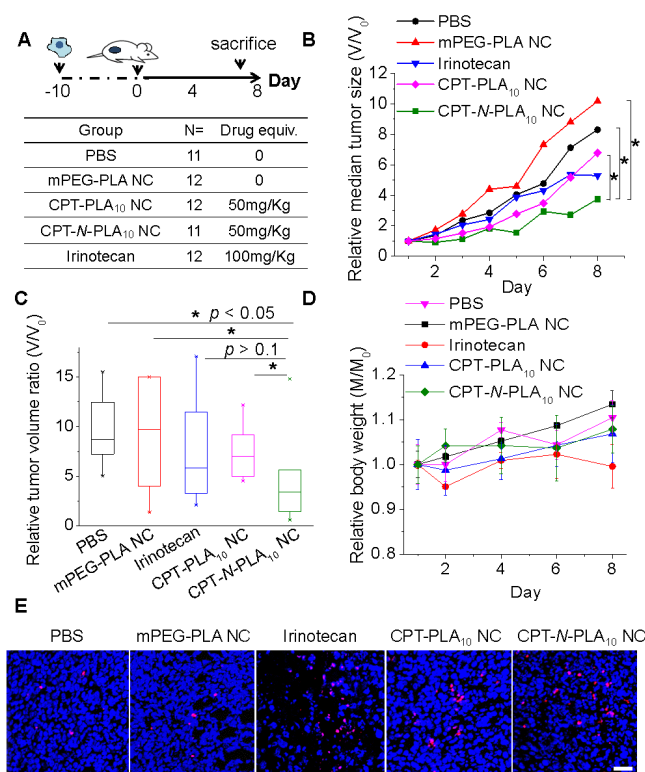


Figure 5. *In vivo* tumor reduction study. (A) Experimental procedures of the study. (B) Delay and inhibition of LLC (Lewis lung carcinoma) tumor growth in C57BL/6 mice with different treatments (PEGylated CPT-LA₁₀ NC, PEGylated CPT-N-LA₁₀ NC, irinotecan, mPEG-PLA NC, and PBS), N=6. Data are presented as relative median tumor size (V/V₀, compare to the tumor volume at day 0). (C) Box plot of LLC tumor growth in C57BL/6 mice at day 8, after treated with PEGylated CPT-LA NC, PEGylated CPT-N-LA NC, irinotecan, mPEG-PLA NC, and PBS at day 0. Statistical properties of relative tumor volume ratio (V/V₀, compare to the tumor volume at day 0) shown in box plot are as follows: box (median with 25/75% percentile), whisker (5/95% percentile), and asterisks (maximum/minimum). Univariate differences between the groups were assessed with Mann-Whitney U test. $P < 0.05$ is considered statistically significant. (D) Relative body weight (M/M₀) monitoring over the study (M: body weight monitored during the study; M₀: body weight monitored at day 0). (E) Representative deoxynucleotidyl transferase-mediated deoxyuridine triphosphate nick end (TUNEL) staining sections of LLC tumors with all treatments (PEGylated CPT-LA₁₀ NC, PEGylated CPT-N-LA₁₀ NC, irinotecan, mPEG-PLA NC, and PBS). Scale bar: 40 μ m.

Table 1Polymerization of LA mediated by CPT-*N*-OH and (BDI-EI)ZnN(TMS)₂.

| Entry ^a | Name | [M]/[Cat.] | Conv (%) ^b | M_n cal ($\times 10^3$ g/mol) | M_n ($\times 10^3$ g/mol) ^c | MWD (M_w/M_n) ^c |
|--------------------|-----------------------------------|------------|-----------------------|-------------------------------------|--|-----------------------------------|
| 1 | CPT- <i>N</i> -PLA ₂₀₀ | 200/1 | >98 | 29.2 | 28.9 | 1.09 |
| 2 | CPT- <i>N</i> -PLA ₁₀₀ | 100/1 | >98 | 14.9 | 15.7 | 1.13 |
| 3 | CPT- <i>N</i> -PLA ₅₀ | 50/1 | >98 | 7.6 | 7.9 | 1.17 |
| 4 | CPT- <i>N</i> -PLA ₁₀ | 10/1 | >98 | 1.9 | 1.4 | 1.23 |

^a All reactions were performed in the glovebox. Abbreviation: Conv. (%) = conversion of monomer %, MWD = Molecular weight distribution.

^b Determined by FT-IR by monitoring the disappearance of the LA peak at 1772 cm⁻¹.

^c Determined by gel permeation chromatography (GPC) and MALDI-TOF MS analysis.

Table 2

Characterization of CPT-*N*-PLA NC prepared by LA polymerization mediated by (BDI-EI)ZnN(TMS)₂ catalyst^a

| Entry ^a | Name | M/I ratio | Eff (%) ^b | Loading (%) ^c | Size (nm) ^d | PDI ^e |
|--------------------|--------------------------------------|-----------|----------------------|--------------------------|------------------------|------------------|
| 1 | CPT- <i>N</i> -PLA ₁₀₀ NC | 100 | >95 | 2.3 | 82 | 0.06 |
| 2 | CPT- <i>N</i> -PLA ₅₀ NC | 50 | >95 | 4.6 | 89 | 0.09 |
| 3 | CPT- <i>N</i> -PLA ₁₀ NC | 10 | >95 | 18.5 | 73 | 0.12 |

^a Abbreviation: NC = Nanoconjugates; M/I = monomer/initiator ratio; Eff = incorporation efficiency, the percent of initiator utilized in the initiation of LA polymerization; PDI = polydispersity derived from particle sizing using DLS. NCs are named as CPT-*N*-PLA_M/I.

^b the data was based on the reversed-phase HPLC analysis of unincorporated drug.

^c the data was based on the reversed-phase HPLC analysis of unincorporated drug.

^d characterized by DLS.

^e characterized by DLS.